Surface modification of GaAs(110) by low-energy ion irradiation

H. Gnaser, B. Heinz, W. Bock, and H. Oechsner

Fachbereich Physik and Institut für Oberflächen- und Schichtanalytik, Universität Kaiserslautern, D-67663 Kaiserslautern, Germany

(Received 18 July 1995)

The GaAs(110) surface was exposed to normal-incidence Ar^+ ion bombardment at energies ranging from 200 eV to 3 keV. The structural, electronic, and compositional modifications induced were monitored by low-energy electron diffraction, electron energy-loss spectroscopy (EELS), and by Auger-electron spectroscopy for different flux densities, accumulated fluences, and specimen temperatures. The fluences necessary for the amorphization of the near-surface region at room temperature amount to some 1×10^{15} Ar^+/cm^2 and increase both with decreasing flux density and with decreasing impact energy, the latter effect being very pronounced below 1 keV. The alterations of the electronic states as inferred from EELS exhibit a similar fluence dependence but are less sensitive to the bombardment energy. Prolonged ion irradiation causes an As depletion of the surface which saturates at fluences $\geq 1 \times 10^{16}$ Ar^+/cm^2, again dependent on the impact energy and flux density. The steady-state Ga/As surface concentration ratio $(c_{Ga}/c_{As})_\infty$ is 1.25 (relative to the bulk composition) at 200 eV and *increases* to ~ 1.45 at 3 keV. These surface composition changes are *reduced* for ion bombardment at elevated specimen temperatures and almost no variations are observed with the sample held at 730 K.

INTRODUCTION

Contrary to most metals, crystalline semiconductors are known[1] to readily amorphize under energetic-ion irradiation at room temperature. This destruction of the crystalline order usually also exerts a tremendous influence on the electronic properties. These processes have been studied[2] extensively for high ion energies (upper keV range), mostly as a means of controlled dopant introduction for electronic device applications; on the other hand, data for low-energy ions (~ 100 eV to 1 keV) are very limited[3] (despite the fact that, historically, low-energy ion bombardment followed by annealing was very early recognized as an effective means[4] for preparing atomically clean surfaces and these experiments outdate most others in this field). At these low-impact energies, the surface is expected to play a significant role in the interactions which occur.[3] Furthermore, in this regime ions are near the threshold for creating atomic displacements in crystals. Due to the lower coordination of surface atoms, an energy region might exist where surface displacements can occur without producing concurrent bulk defects.[3] While bulk displacement energies are rather poorly known,[5] there is hardly any information available on surface displacement energies.[3] Closely related, of course, to these threshold values is the absolute number of displacements at the surface and in the bulk for low-energy ion irradiation. Recent work employing scanning tunneling microscopy[6-10] has provided considerable information on defect formation on surfaces.

Apart from these basic considerations, low-energy ion beams are of interest for assisting thin-film growth.[11] Also, on growing surfaces ions can enhance dopant incorporation[12] and have been used as a direct means to deposit epitaxial films.[13] Recently, ion beams were used to control the surface morphology during epitaxial growth[3] and led to a rapid smoothening of semiconductor surfaces. For such applications low energies appear mandatory; quite often, the controlled production of surface defects which mediate epitaxial growth processes and the minimization (or even elimination) of bulk defects might be the ultimate goal.

The present experiments aim to address, from a fundamental viewpoint, some of the questions outlined above (see also Ref. 14). The modification of GaAs(110) surfaces caused by low-energy ion impact, effecting an impact-energy and fluence-dependent production of atomic displacements, was investigated. The latter became manifest in electron-diffraction studies; associated modifications of electronic surface and bulk states were monitored from the changes of transitions involving those states, and the surface composition variations were recorded in dependence on different irradiation parameters. Specifically, crystalline surfaces of GaAs(110) were subjected to Ar^+ ion bombardment in the energy range from 200 eV to 3 keV. The bombardment-induced amorphization and related electronic modifications were monitored by means of low-energy electron diffraction (LEED) and electron energy-loss spectroscopy (EELS). Surface composition changes due to ion irradiation were investigated by Auger-electron spectroscopy (AES). For appropriate experimental parameters, these techniques are extremely surface sensitive,[15] and therefore enable the detection of structural, electronic, and compositional changes induced by ion impact in the topmost atomic layers of the solid. This work thus constitutes an extension of our related studies[14] on the elemental semiconductors Si(111) and Ge(100).

EXPERIMENT

The experimental setup employed for these investigations is described in detail in Ref. 14. The modification of crystalline GaAs(110) surfaces due to low-energy ion

bombardment was studied by means of LEED, EELS, and AES. These experiments were performed in an ion-getter-pumped UHV chamber with a base pressure of $\sim 1 \times 10^{-10}$ mbar.[14] Ion beams were produced in a standard electron-impact ion gun. Typical ion flux densities were $1-16 \times 10^{12}$ Ar$^+$/cm^2 s. Electron-diffraction data were obtained with a standard four-grid retarding field LEED optics (Phi 15-120) and images were recorded on 35-mm BW film. Typical primary electron currents were 1 μA. The EELS and AES measurements were performed in a cylindrical-mirror energy analyzer with a coaxial electron gun (Phi 10-155) and an energy resolution of 0.6%. At a typical beam energy of about 100 eV, the electron beam (~ 1 μA current) had a spot size of ~ 130 μm and an energy width of 1.4 eV. The EELS data were recorded as the second derivative by means of lock-in techniques. The specimen manipulator was equipped with a Faraday cup for current (density) measurements, a resistively heated tungsten filament for sample heating by radiation and, in some cases, also by electron impact, and a thermocouple for controlling the sample temperature.

The samples utilized were n-doped GaAs(110) single-crystal wafers. Prior to their insertion into the vacuum chamber, they were etched in 5% Br-methanol solution[16,17] and subsequently rinsed in ethanol and distilled water. The remaining surface contaminants (mostly carbon, oxygen, and, to a lesser extent, nitrogen, chlorine, and sulfur) were removed by repeated ion bombardment and annealing (at 800 K) cycles. Upon this procedure no impurities were detectable by AES and the LEED images were sharp and without any noticeable background. The clean, crystalline surface was then exposed to normal-incidence ion irradiation by increasing the applied fluence incrementally; LEED images as well as EELS and AES spectra were recorded after each fluence step. This procedure was repeated until the accumulated ion fluence was sufficient for the complete amorphization of the near-surface region, as was evident from the disappearance of all LEED spots, and an equilibrium state of the EELS and AES peak heights was reached. The ion flux densities j_p used were in the range from 1×10^{12} to 16×10^{12} Ar$^+$ ions/cm^2 s. The crystalline structure was restored by annealing the specimens at a temperature of about 800 K for 2 min.

RESULTS AND DISCUSSION

The GaAs(110) surface is different from the Si and Ge surfaces investigated in Ref. 14 in that it does *not* exhibit a reconstruction. In contrast to other low-index surfaces of GaAs, the (110) surface is nonpolar and thus contains an equal number of Ga and As atoms. Detailed LEED investigations[18,19] revealed, however, that the atoms of the topmost layers are slightly shifted relative to the underlying bulk layers, i.e., the surface layer is relaxed, which results in an energetically more favorable condition.[19] This vertical cation-anion shear represents about 30% of the original interlayer spacing ($d = 1.999$ Å) and causes a rotation of the Ga-As bond angle by about 27° from the ideal surface plane.[20] The atoms at the surface experience, due to the missing bonding partners, a rear-

rangement of their binding-orbital configuration. The As atoms (lying slightly above the Ga atoms on the relaxed surface) now have three p-like orbitals (roughly at angles of 90° to each other) which form the bond to their neighbors and a doubly occupied dangling-bond state which lies in the valence band. The Ga atoms have three binding sp^2 orbitals and an empty dangling bond in the conduction band of the crystal.[21]

In the following, ion-bombardment-induced structural, electronic, and compositional modifications of the GaAs(110) surface will be investigated by means of low-energy electron diffraction, electron energy-loss spectroscopy, and Auger-electron spectroscopy.

Low-energy electron diffraction

In this section the energy dependence of the ion fluence necessary to amorphize the near-surface region of GaAs(110) single crystals will be reported. The fluence required for the complete extinction of the LEED pattern will be called amorphization fluence Φ_a in the following. The GaAs surfaces were exposed, at different impact energies, to Ar$^+$ flux densities of 4×10^{12}, 8×10^{12}, and 16×10^{12} cm^{-2} s^{-1}, respectively; with an increasing total fluence the LEED spot intensities gradually diminish until they finally disappear. From such exposure series, the values of Φ_a were derived for different bombarding energies. Apart from the impact energy, a dependence of Φ_a on the ion flux density was also observed. These results are shown in Fig. 1 which plots the scaling of Φ_a with impact energy and j_p as parameter. Above an impact energy of ~ 1.5 keV, Φ_a is roughly constant, but rises steeply below that value. Two major differences are apparent for GaAs as compared to the elemental semiconductors Si and Ge.[14] First, Φ_a is strongly dependent on the ion flux density,[22] in a way that decreasing the latter increases the value of Φ_a at a given bombarding energy. Below $E = 1$ keV no amorphization is reached for the current densities accessible in this work. For a flux densi-
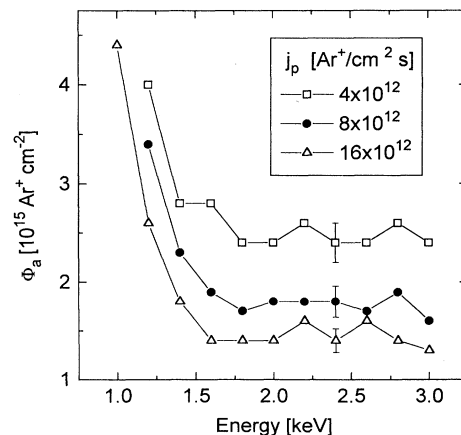

FIG. 1. Amorphization fluence Φ_a as derived from LEED versus the bombarding energy. The parameter is the ion flux density.

ty of 1×10^{12} ions/cm^2 s (or less), amorphization of the GaAs(110) surface could not be reached for the employed impact energies, even for total fluences in excess of 10^{16} ions/cm^2. Second, the values of Φ_a (cf. Fig. 1) for GaAs(110) are about an order of magnitude higher than the corresponding ones reported[14] for Si and Ge single crystals bombarded under similar conditions.

Since $\langle 110 \rangle$ constitutes the most open lattice direction in diamond and zinc blende crystals, the possible influence of crystalline transparency on Φ_a was checked by determining the amorphization fluences with the specimen tilted by $8°\pm1°$ off the surface normal. The derived values of Φ_a were found to be identical to those for normal-incidence ion bombardment. It is concluded thus that enhanced ion penetration is of no concern in the energy regime ($E \leq 3$ keV) investigated.

Recent experiments by Weaver et al.[23] on the defect production in GaAs(110) using thermal He scattering demonstrated that apart from thermal annealing another process can reduce the number of defects. In this picture, bombardment-induced recombination of defects with weakly bonded adatoms at the surface can occur. Due to ion impact the latter gain sufficient mobility for such a process to take place. The data in Fig. 1, therefore, indicate that annealing processes can occur sufficiently rapidly to counterbalance the production of ion-bombardment-created defects. If, in addition, the creation rate is too low (at low current densities), the crystalline structure remains largely intact (i.e., at least on a scale sufficient to produce LEED images). To verify this possibility, additional experiments at different sample temperatures during bombardment would be desirable.

Electron energy-loss spectroscopy

The local density of states at the surface is modified by a distortion or destruction of the crystalline lattice.[24] Thus ion-bombardment-induced surface modifications can be monitored using low-energy electrons which, in the energy range from 10 to about 200 eV, are very surface sensitive. Similar to the Si and Ge surfaces described in Ref. 14, EELS was employed also for GaAs(110) to investigate those irradiation effects. Inelastically scattered electrons provide information on characteristic energy losses due to collective excitations or interband (intraband) transitions. The former result from the excitation of valence-band electrons (bulk and surface plasmons); the latter are a consequence of electron transitions between different energy states, both within a band or among different bands. The surface relaxation causes the development of additional dangling-bond and backbond states (see above) which can take part in electronic transitions.

Figure 2(a) shows a typical energy-loss spectrum obtained from a crystalline GaAs(110) surface using 80-eV electrons for excitation. The data are recorded as the negative second derivative by means of lock-in techniques and the energy loss is plotted relative to the peak of the elastically scattered electrons. Table I lists the energy loss of the most prominent peaks [labeled in Fig. 2(a)] and the associated transitions which are well documented in
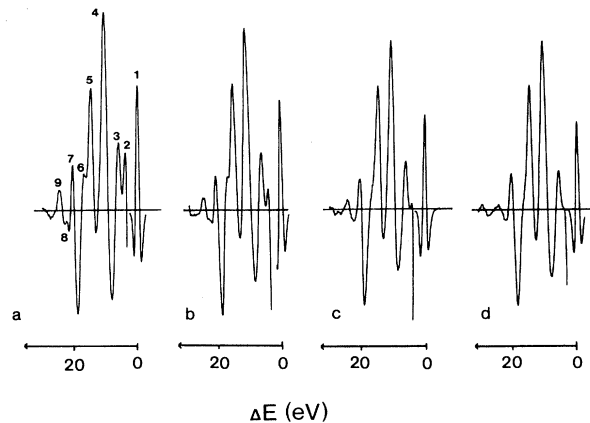

FIG. 2. EELS spectra of GaAs(110) recorded as the negative second derivative versus the energy loss relative to the elastic peak [labeled "1" in (a)]. The energy loss and the respective transitions corresponding to the peaks designated in (a) are compiled in Table I. Electron energy was 80 eV and the current 1.7 μA. The spectra were taken from a pristine GaAs(110) surface (a) and upon bombardment with 3-keV Ar$^+$ at fluences of 5×10^{13} cm^{-2} (b), 3×10^{14} cm^{-2} (c), and 2×10^{15} cm^{-2} (d).

the literature. The changes of EELS spectra due to ion bombardment are depicted in Figs. 2(b)–2(d). Since variations in peak heights were observed already for rather low fluences ($\sim 5 \times 10^{13}$ ions/cm^2), ion irradiation was done at a flux density of 1×10^{12} Ar$^+$ ions/cm^2 s. Some data taken at higher densities produced similar fluence-dependent changes of the EELS spectra, but low-fluence features could not be followed as accurately.

Since no changes in peak shape and width were observed with ion bombardment, the peak heights in the doubly differentiated spectra can be assumed to represent the actual intensities of the backscattered electrons. The normalized peak heights of selected peaks are plotted in Fig. 3 as a function of bombarding fluence. For several transitions, drastic variations are found at comparatively low fluences ($< 10^{14}$ cm^{-2}) and the signals level off to constant values at about 1×10^{15} ions/cm^2. It appears that the qualitative shape of these fluence-dependence curves are essentially *independent* of impact energy, even for bombardment energies as low as 200 eV (the lower limit accessible experimentally). By contrast, LEED images did not show any irradiation-related changes below $E \sim 1$ keV. The EELS data nevertheless demonstrate that some defect production in the near-surface layers does occur and they exemplify the sensitivity of this technique.

The most pronounced variations in signal heights are found for peak Nos. 2 and 9 (see Fig. 2). Two processes can contribute to the former (cf. Table I). The complete extinction upon ion bombardment indicates, however, that the transition between Ga and As dangling-bond states dominates here. This is because, as discussed in Refs. 30 and 31, the Ga surface state responds very sensitively to changes of the Ga-As bond angle at the relaxed GaAs(110) surface; very likely, this angle is readily modified due to ion impact and the associated relocation

TABLE I. Energy-loss peaks shown and labeled in Fig. 2(a) with their position (ΔE) relative to the elastic peak and the electronic transitions.

Peak no.	ΔE [eV]	Transition
1	0	Elastic peak
2	3.5	As dangling bond→Ga dangling bond (Ref. 25) and bulk valence to conduction band (Ref. 26)
3	5.8	Bulk valence band to conduction band (Refs. 25 and 27)
4	10.6	Surface plasmon (Ref. 25)
5	15.5	Bulk plasmon (Refs. 25 and 27)
6	18.0	As backbond→Ga dangling bond (Ref. 26)
7	20.0	$3d$ core electron→excitonic surface state (Refs. 28 and 29)
8	21.6	$3d$ core electron→Ga dangling bond (Ref. 26)
9	24.1	$3d$ core electron→conduction band (Ref. 25).

of (surface) atoms. As peak No. 2 disappears at fluences ranging from 6 to 10×10^{14} Ar$^+$ cm^{-2} (which is slightly less than the number of atoms per monolayer), it may be concluded that each impinging Ar ion creates at least one (and possibly more) defect site in the surface. Peak Nos. 6 and 8 also involve the excitation into a Ga dangling-bond state and, not surprisingly, react very prominently to ion bombardment (see Fig. 2). Due to their intrinsic weakness even in the crystalline state, their signal evolution with increasing fluence could not be recorded in a quantitative manner.

Auger-electron spectroscopy

Compositional changes induced by ion bombardment on the GaAs(110) surface were monitored by means of Auger-electron spectroscopy. Specifically, the dependence of the Ga and As surface concentrations on the Ar$^+$ impact energy, the current density, and the ion fluence were investigated. In addition, some measurements were performed at elevated sample temperatures. Normal-incidence ion bombardment with energies in the
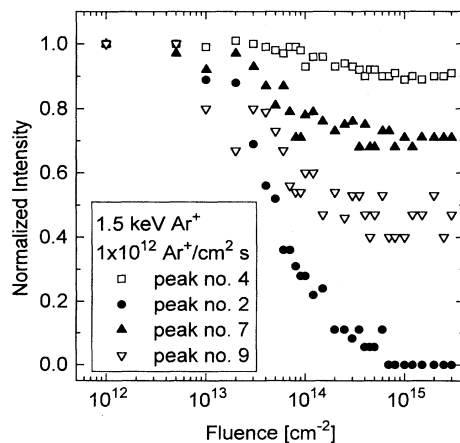
range from 200 eV to 3 keV was done at three different flux densities ($j_p = 1$, 4, and 16×10^{12} Ar$^+$/cm^2 s); the applied fluence was increased in increments of 5×10^{14} ions/cm^2 until a total fluence of 1×10^{16} cm^{-2} was accumulated. AES spectra were recorded after each step; excitation was done with 3-keV electrons (currents ~2 μA) and the low-energy AES peaks of As (31 eV) and of Ga (55 eV) were monitored as the peak-to-peak amplitude in the (singly) differentiated spectrum. Upon reaching the maximum fluence, the original sample composition could be restored by annealing at 800 K.

For two impact energies, Fig. 4 shows the dependence of the Ga/As intensity ratio as a function of fluence, with the flux density as the parameter; the data thus represent

FIG. 3. EELS peak heights normalized to the values of the unbombarded surface vs ion fluence for 1.5-keV Ar$^+$ ion impact on GaAs(110).
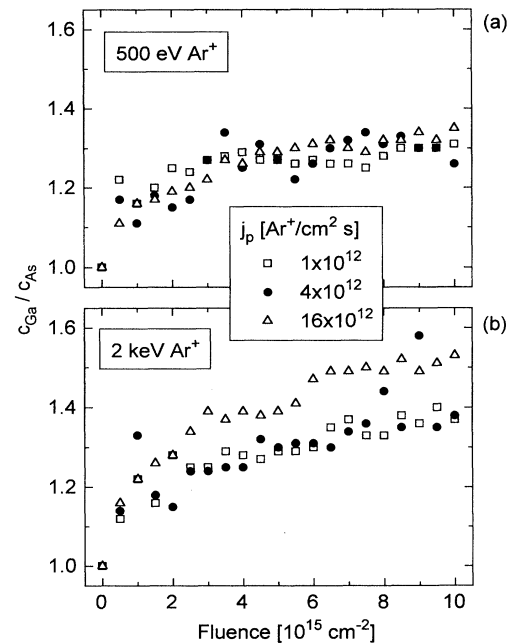

FIG. 4. Ga/As surface concentration ratios derived from the respective low-energy AES peaks versus the fluence for the bombardment of GaAs(110) by 0.5-keV Ar$^+$ (a) and by 2-keV Ar$^+$ (b). The parameter is the ion flux density.

the gradual variation of the surface composition due to ion irradiation. Because of their low energy (and the associated short mean-free-path length), the AES electrons probe a depth of about 2–3 ML.[32,33] The average penetration depth of Ar^+ ions in GaAs amounts to ~ 10 Å at 200 eV and increases to roughly 40 Å at 3 keV.[34] Thus, at the lowest bombarding energies, the modified sample region is comparable to the information depth, but becomes much larger at the higher energies.

Figure 4 exemplifies the general tendencies of the results: (i) With increasing bombarding fluence the surface is enriched in Ga and an equilibrium is reached for a fluence $\sim 10^{16}$ cm^{-2} for low impact energies and, judging from an extrapolation, at some 10^{16} cm^{-2} for $E > 1$ keV. (ii) The near-surface Ga enrichment increases with increasing impact energy. (iii) While at low bombarding energy the steady-state enrichment is independent of the current density, it appears to increase with flux density above ~ 1 keV; this observation is, however, less clear cut in that the data for the intermediate flux density (4×10^{12} cm^{-2} s^{-1}) exhibit considerable scatter in this energy regime. It is worthwhile to note that the absolute AES signals of Ga and As produce a different fluence dependence: for all energies and fluxes, the As signal remains roughly constant, but the Ga intensity rises with increasing fluence.

From the data in Fig. 4 and similar ones for the other impact energies, the steady-state surface-concentration ratios $(c_{Ga}/c_{As})_\infty$ were derived. For $E \geq 1$ keV an extrapolation to higher fluences was carried out to obtain an estimate for the equilibrium composition. The values of $(c_{Ga}/c_{As})_\infty$ are depicted in Fig. 5 versus the Ar^+ bombarding energy. As mentioned, the equilibrium ratio is found to increase with E and, for higher energies, tends to be higher for higher flux densities. It is noted that the highest ratio corresponds to Ga and As surface concentrations of 59% and 41%, respectively. To investigate the influence of the AES probing depth, two bombardment series (at 0.2 and 3 keV) were done monitoring the
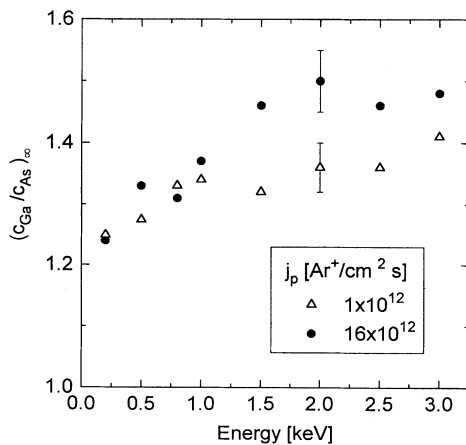
high-energy Ga and As Auger electrons; their energies of, respectively, 1070 and 1228 eV translate into mean-free-path lengths of about 20 Å.[33] Qualitatively, these experiments produce the same fluence-dependent variation of the Ga/As composition, but the steady-state ratio $(c_{Ga}/c_{As})_\infty$ is lower (~ 1.1 and 1.2 for 0.2-keV and 3-keV Ar^+ impact, respectively) than the values observed for the low-energy AES peaks (1.2 and 1.4; see Fig. 5).

The steady-state compositions determined in this work are in good agreement with previous AES data[35–39] and generally indicate a distinct Ga *enrichment* over the depth probed by low- and high-energy AES peaks, which increases with increasing impact energy and is apparently independent of the incidence angle.[39] A quantitative comparison of the reported $(c_{Ga}/c_{As})_\infty$ values is difficult due to the different bombarding flux densities (cf. Fig. 5) and the differences in probing depth of the high-energy AES lines used in most previous work.[37–39] A discrepancy in the literature data concerns the depth variation of the As depletion and Ga enrichment. Some results[22,38] indicate an enhanced As concentration in the *outermost* layer of ion-bombarded GaAs. The latter observation strongly points to a surface segregation of As atoms and an As depletion in the subsurface layers, extending at least to the depth probed by (high-energy) Auger electrons (i.e., some 20 Å). The apparently high mobility of arsenic implied by such a segregation is reminiscent of the lack of a complete amorphization observed in the LEED data at low impact energies and/or low current densities. In that context it was argued that thermally activated processes cause a rapid annealing of defects even at room temperature.[23] These authors, using thermal-atom scattering, argue that 600-eV Ar^+ ion bombardment of GaAs(110) at $T = 300$ K results in 2.3 to 5 defects, approximately one of which is a target adatom, which can make a few jumps before freezing. They hypothesize, furthermore, that above 600 K adatoms remain mobile until recombining with vacancies or forming adatom clusters and that at and above 700 K complete thermal annealing of the created defects occurs.

These arguments are in broad agreement with much earlier data of Anderson and Wehner,[40] who studied the temperature dependence of sputtered-atom ejection patterns from semiconductors. They observed that below a critical impact energy E_c spot patterns persist, which was taken as an indication of the crystallinity of the specimen. Also, above a threshold temperature T_a the value of E_c steeply increases, to the extent that the sample remains crystalline for all but the very highest bombarding energies. For GaAs, $T_a \sim 400$ K and E_c in the range 100 to 300 eV were determined.[41] It is noted, however, that these authors employed current densities at least two orders of magnitude larger than those of the present work. Anderson and Wehner tried to model their findings from a balance of defect production and the concurrent annealing of these defects. Explicitly, an equilibrium defect density N_0 [defects/cm^2] is given[40]

FIG. 5. Steady-state Ga/As surface-concentration ratio $(c_{Ga}/c_{As})_\infty$ as a function of Ar^+ impact energy for two ion flux densities.

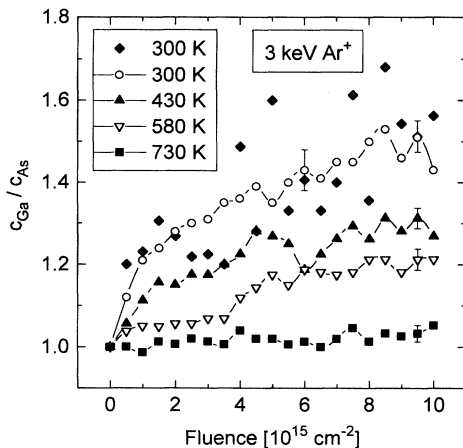$$N_0 = \frac{j_p \beta(E)}{\nu \exp(-E_a/kT)}, \tag{1}$$

FIG. 6. Ga/As concentration ratio (derived from low-energy AES) versus fluence for 3-keV Ar^+ ion bombardment at the sample temperatures indicated. The ion flux density was 4×10^{12} $cm^{-2}s^{-1}$ in all cases with the exception of one of the 300-K data (open circles) which was taken at 16×10^{12} $cm^{-2}s^{-1}$.

where j_p is the flux density, $\beta(E)$ is the number of defects produced per ion of energy E, ν is the atom jump frequency, and E_a is an activation energy for defect migration. From this approach they derived[40,41] values of $E_a \sim 0.7$–0.8 eV for various III/V semiconductors and slightly larger values for Ge (1.1 eV) and Si (1.4 eV).

To study the possible influence of thermal processes, compositional variations were monitored at different sample temperatures during ion bombardment. Figure 6 shows the gradual change of the Ga/As surface-concentration ratio with increasing fluence of 3-keV Ar^+ ions at various elevated temperatures. Compared to the room-temperature bombardments, increasing the sample temperature drastically reduces the observed Ga enrichment, until, at about 730 K, essentially no compositional changes are observed upon ion bombardment. These data are in agreement with the tendencies in the aforementioned investigations.[23]

In a related experiment, Singer, Murday, and Cooper[22] monitored the (high-energy) AES intensity ratio Ga/As as a function of ion current density at various sample temperatures and found that increasing the current density at a given temperature beyond a critical value results in a rapid increase of the Ga/As intensity ratio. This limiting current density rises with the temperature. These authors thus conclude that, depending on j_p and T, two regimes may be discerned, one where the Ga/As stoichiometry is largely preserved (at high T and/or low j_p) and a second where Ga enrichment occurs for low T or large j_p. For 2-keV Ar^+ impact and the current density used to obtain the data depicted in Fig. 6 (4×10^{12} $cm^{-2}s^{-1}$), they derive a limiting temperature of about 330 K. The results in Fig. 6 indicate in fact that in the temperature range between 300 and 430 K a pronounced change in Ga/As composition takes place. The consider-

able scatter of the data for the specific value (4×10^{12} Ar^+/cm^2s) of the ion flux density [cf. Figs. 4(b) and 6] indicates that, at $T = 300$ K, j_p falls into this transition regime (from stoichiometric to nonstoichiometric composition) mentioned above. To assess this option, the defect density N_0 is evaluated according to the approach of Anderson and Wehner,[40] Eq. (1), using $E_a = 1$ eV as determined by Singer, Murday, and Cooper,[22] $\beta = 3$ (see Ref. 23), and $\nu = 10^{13}$ s^{-1}.[42] For $j_p = 4 \times 10^{12}$ ions/cm^2s, $N_0 = 8.2 \times 10^{16}$ cm^{-2} at $T = 300$ K, but falls to 3.2×10^{14} and 5.1×10^{12} cm^{-2} for $T = 350$ and 400 K, respectively. Thus, in agreement with the data shown in Fig. 6, a drastic reduction of defects (through annealing) occurs in this temperature interval; this enhanced annealing apparently causes the Ga/As concentration ratio to approach the bulk stoichiometry at elevated temperatures.

CONCLUSIONS

Summarizing the ion-bombardment-induced modifications observed on GaAs(110) surfaces, a prominent feature is noted: A high mobility of target atoms appears to balance the production of defects and the relocation of atoms; this mobility depends sensitively on the sample temperature. Experimentally, it is manifested in a dependence on the flux density (i.e., the defect production rate) of both the amorphization fluence (as derived from electron diffraction) and the Ga/As composition (determined from AES). In the latter case, it is also noticed directly from a variation of the specimen temperature. While for GaAs these effects take place already at room temperature, for the elemental semiconductors Si and Ge they may become apparent only at much higher temperatures [the lack of an amorphization of Ge(100) subjected to 100-eV Ar^+ impact[14] might, in fact, be an indication for the occurrence of such processes also for this material]. These differences have their origin in the much lower activation energy for atom and defect migration in GaAs ($E_a \sim 1$ eV or less[22,40]) as compared to Ge (~ 1.1 eV) and Si (1.4 eV). This high mobility might also have a decisive influence on the (somewhat surprising) finding that the Ga enrichment *increases* with *increasing* bombardment energy (see Figs. 4 and 5). If the compositional variations were solely due to preferential sputtering, the reversed dependence would be expected.[43–45] The probing depth of the low-energy Auger electrons is much shallower (~ 6 Å) than the Ar^+ range and the thickness of the damaged (altered) layer. The latter was determined[46] from medium-energy ion scattering to increase from 30 Å at 0.5-keV Ar^+ impact to about 65 Å at 3 keV and is thus roughly twice the projected range of Ar^+ ions in GaAs.[34] The results indicate, therefore, that the As relocation out of the surface layer (probed by AES) and the possible replacement by Ga atoms increases in efficiency with the enlargement of the damaged volume, that is to say, with increasing energy. These transport processes are facilitated by the comparatively high atomic mobility in this kind of specimen.

[1]See, for example, *Point Defects in Solids,* edited by J. H. Crawford and L. M. Slifkin (Plenum, New York, 1975), Vol. 2.

[2]J. W. Corbett, J. P. Karins, and T. Y. Tan, Nucl. Instrum. Methods **182/183**, 457 (1981).

[3]S. T. Picraux, D. K. Brice, K. M. Horn, J. Y. Tsao, and E. Chason, Nucl. Instrum. Methods B **48**, 414 (1990).

[4]H. E. Farnsworth, R. E. Schlier, T. H. George, and R. M. Burger, J. Appl. Phys. **29**, 1150 (1958).

[5]J. W. Corbett and J. C. Bourgoin, in *Point Defects in Solids* (Ref. 1), p. 1.

[6]T. Michely and G. Comsa, J. Vac. Sci. Technol. B **9**, 862 (1991); Nucl. Instrum. Methods B **82**, 207 (1992).

[7]P. Bedrossian, J. E. Houston, J. Y. Tsao, E. Chason, and S. T. Picraux, Phys. Rev. Lett. **67**, 124 (1991).

[8]H. J. W. Zandvliet, H. B. Elswijk, E. J. van Loenen, and I. S. T. Tong, Phys. Rev. B **46**, 7581 (1992).

[9]J. C. Girard, Y. Samson, S. Gauthier, S. Rousset, and J. Klein, Surf. Sci. **302**, 73 (1994).

[10]R. J. Pechman, X.-S. Wang, and J. H. Weaver, Phys. Rev. B **51**, 10 929 (1995).

[11]*Ion Beam Assisted Film Growth,* edited by T. Itoh (Elsevier, Amsterdam, 1989).

[12]J. L. Zilko and J. E. Greene, J. Appl. Phys. **51**, 1549 (1980).

[13]B. R. Appleton, S. J. Pennycook, R. A. Zuhr, N. Herbots, and T. S Noggle, Nucl. Instrum. Methods B **19/20**, 975 (1987).

[14]W. Bock, H. Gnaser, and H. Oechsner, Surf. Sci. **282**, 333 (1993).

[15]D. P. Woodruff and T. A. Delchar, *Modern Techniques of Surface Science* (Cambridge University Press, Cambridge, 1986).

[16]A. U. MacRae, Surf. Sci. **4**, 247 (1966).

[17]A. F. Bogenschütz, *Ätzpraxis für Halbleiter* (Hanser, München, 1967).

[18]A. U. MacRae and G. W. Gobeli, J. Appl. Phys. **35**, 1629 (1964).

[19]A. Kahn, Surf. Sci. Rep. **3**, 193 (1983).

[20]M. W. Puga, G. Xu, and S. Y. Tong, Surf. Sci. **164**, L789 (1985).

[21]W. E. Spicer, P. Pianetta, I. Lindau, and P. W. Chye, J. Vac. Sci. Technol. **14**, 885 (1977).

[22]J. L. Singer, J. S. Murday, and L. R. Cooper, Surf. Sci. **108**, 7 (1981).

[23]B. D. Weaver, D. R. Frankl, R. Blumenthal, and N. Winograd, Surf. Sci. **222**, 464 (1989).

[24]R. Ludeke and L. Esaki, Surf. Sci. **47**, 132 (1975).

[25]H. Lüth and G. J. Russell, Surf. Sci. **45**, 329 (1974).

[26]J. van Laar, A. Huijser, and T. L. van Rooy, J. Vac. Sci. Technol. **14**, 894 (1977).

[27]C. v. Festenberg, Z. Phys. **227**, 453 (1969).

[28]W. Gudat and D. E. Eastman, J. Vac. Sci. Technol. **13**, 831 (1976).

[29]D. E. Eastman, T. C. Chiang, P. Heimann, and F. J. Himpsel, Phys. Rev. Lett. **45**, 656 (1980).

[30]R. Ludeke and A. Koma, J. Vac. Sci. Technol. **13**, 241 (1976).

[31]J. R. Chekikowsky and M. L. Cohen, Phys. Rev. B **20**, 4150 (1979).

[32]P. Pianetta, I. Lindau, C. M. Garner, and W. E. Spicer, Phys. Rev. B **18**, 2792 (1978).

[33]W. Ranke and K. Jacobi, Surf. Sci. **47**, 525 (1975).

[34]J. F. Ziegler, J. P. Biersack, and U. Littmark, *The Stopping and Range of Ions in Matter* (Pergamon, New York, 1985), Vol. 1.

[35]A. van Oostrom, J. Vac. Sci. Technol. **13**, 224 (1976).

[36]I. L. Singer, J. S. Murday, and J. Comas, J. Vac. Sci. Technol. **18**, 161 (1982).

[37]Y. X. Wang and P. H. Holloway, J. Vac. Sci. Technol. A **2**, 567 (1984).

[38]S. Valeri and M. Lolli, Surf. Interface Anal. **16**, 59 (1990).

[39]J. B. Malherbe, W. O. Barnard, I. Le R. Strydom, and C. W. Louw, Surf. Interface Anal. **18**, 491 (1992).

[40]G. S. Anderson and G. K. Wehner, Surf. Sci. **2**, 367 (1964).

[41]G. S. Anderson, J. Appl. Phys. **37**, 3455 (1966).

[42]H. C. Casey and G. L. Pearson, in *Point Defects in Solids* (Ref. 1), Vol. 2, p. 163.

[43]G. Betz and G. K. Wehner, in *Sputtering by Particle Bombardment,* edited by R. Behrisch (Springer, Berlin, 1983), Vol. II, p. 11.

[44]H. H. Andersen, in *Ion Implantation and Beam Processing,* edited by J. S. Williams and J. M. Poate (Academic, Sydney, 1984), p. 127.

[45]N. Q. Lam, Scanning Microsc. Suppl. **4**, 311 (1990).

[46]I. Konomi, A. Kawano, and Y. Kido, Surf. Sci. **207**, 427 (1989).